Sensors & Transducers, Vol. 184, Issue 1, January 2015, pp. 153-158

Sensors & Transducers

http://www.sensorsportal.com

Design and Development of a Magneto-Optic Sensor for Magnetic Field Measurements

*** Sarbani CHAKRABORTY and Sarita KUMARI**

Department of Electrical and Electronics Engineering, Birla Institute of Technology
Mesra, Ranchi-835215, Jharkhand, India
* Tel.: + 919431129477
* E-mail: schakraborty@bitmesra.ac.in

Received: 31 December 2014 /Accepted: 27 January 2015 /Published: 31 January 2015

Abstract: A magneto-optic sensor is developed using a Terbium Doped Glass (TDG) element as a Faraday rotation sensor and optical fiber as light transmitting and receiving medium. Online LabView based application software is developed to process the sensor output. The system is used to sense the magnetic field of a DC motor field winding in industrial environment. The sensor output is compared with the magnetic flux density variation obtained with a calibrated Hall Magnetic sensor (Gauss Meter). A linear variation of sensor output over wide range of current passing through the field winding is obtained. Further the results show an improved sensitivity of magneto-optic sensor over the Hall sensor. *Copyright © 2015 IFSA Publishing, S. L.*

Keywords: Current measurement, Faraday effect, Magnetic field measurement, Magnetooptic devices, Magnetic sensors, Optical imaging, Polarimetry, Stokes parameters.

1. Introduction

Different technologies are used for measuring magnetic fields. Lion [1] described fundamental description of both mechanical and electrical means for sensing magnetic fields. H. R. Everett and J. E. Lenz [2, 3] have described surveys on magnetic sensor technologies. Induction coil magnetometer [4], Fluxgate magnetic sensor [4], Hall magnetic sensor [5] etc are commercially available magnetic field sensors used for wide ranging applications such as measuring rock magnetism, satellite altitude control system etc.[6] Super-conducting quantum interference device [3], Giant magneto resistance (GMR) magnetic field sensor [7-9] etc are some important developments in magnetic sensor technology. The optical sensors are now-a-days gaining importance since they are free from measurement errors due to various effects like stray electromagnetic effect, capacitive effect, etc., which are observed in many non-optical sensors along with their advantages of electrical isolation, large bandwidth, ease of integration into digital control system, etc. [10–15].

One very important property used in optical sensors is the Faraday rotation of polarized light in a typical solid, liquid or gaseous medium such as glass, quartz, water, and sodium vapor when subjected to a strong magnetic field [16]. Ferrimagnetic materials such as Yttrium Iron Garnet (YIG) ($Y_3Fe_{15}O_{12}$) and ferromagnetic materials such as Iron (Fe), Nickel (Ni) and Gadolinium (Ge) offer highest Faraday rotation but high degree of nonlinearity is also observed in the net Faraday Effect [17]. Large iron garnet crystal is not suitable where sensor linearity is important.

In these materials volumes of equal direction of magnetization (magnetic domains) are formed.

The external magnetic field applied perpendicular to such material cause the domains with magnetization in the direction of the field to grow at the expense of other domains [17]. The net polarization rotation can be approximated using the area ratio between two kinds of domain. The domain size and hence the Faraday rotations depend on the material property as well as sample geometry. Owing to high Faraday rotation these materials are also used in thin film geometry with compensation technique for nonlinearity. The Faraday rotations can be altered by adding mainly rare earth ions. Bismuth (Bi) is commonly added to achieve higher rotations. Jeon et al. showed that Faraday rotation and Verdet constant of Bi-substituted YIG ($Bi_{1.8}Y_{1.2}Fe_5O_{12}$) material can be enhanced to 5.28 deg/mm and 2.63×10^{-2} deg/Oe cm [18]. Some films are made with complete substitution of Bi in place of Y such as the composition $Bi_3Fe_5O_{12}$ or BIG which are commercially used in laser isolators [19]. In magneto-optic current sensors the principle of Faraday rotation is extensively used by using bulk optical element or optical fiber [20-24] as magneto-optic medium. However, there is a constraint in the use of multi-turn optical fiber due to low Verdet constant and inherent intrinsic birefringence and bend-induced linear birefringence effect [25]. This leads to the use of bulk optics in place of optical fiber [26–30]. Chakraborty et al. [31-35] designed and developed magneto-optic sensors using bulk optical material. The diamagnetic materials like SF-57, SiO_2 and BK7 etc. and paramagnetic materials like Terbium Gallium Garnet (TGG) crystal, Terbium doped glass (TDG), etc. used in bulk optics are still being studied by various workers [26–30]. Gillman has observed large rotations in magneto-optic laser isolators at 632 nm wavelength using TGG and Tb-doped glass (TDG) of Verdet constant -134 and -70 rad/ T.m respectively [26]. Mansell et al. have observed that change in optical path length due to thermal expansion is smaller in Hoya FR-5 (TDG) than TGG [28]. Very recently Li et al. have developed Faraday glasses with large size and high performance [29]. Goldring et al. have utilized magneto-optic element for control of polarization [30]. In the present work the design, development and testing of a prototype TDG based magneto-optic sensor is discussed. A comparative study with the performance of Hall sensor is also included.

2. Theory and Analysis

Basic schematic diagram of the magneto-optic measurement set up in transmission mode is shown in Fig. 1. Let the beam incident on the magneto-optic element be linearly polarized with azimuth α_p has intensity I_0. The Stokes vector of the output beam from the analyzer can then be written as

$$S_{out} = I_0 \, M_{ana} \, M_{rot} \, S_{in}, \tag{1}$$

where M_{rot} and M_{ana} are the Mueller matrices [13, Chapter-33] of Faraday rotator and analyzer respectively, and S_{in} is the normalized Stokes vector of the input linearly polarized beam which are given by the following equations

$$M_{rot} = \begin{bmatrix} 1 & 0 & 0 & 0 \\ 0 & \cos 2\theta & -\sin 2\theta & 0 \\ 0 & \sin 2\theta & \cos 2\theta & 0 \\ 0 & 0 & 0 & 1 \end{bmatrix} \tag{2}$$

$$M_{ana} = \frac{1}{2}\begin{bmatrix} 1 & \cos 2\alpha_a & \sin 2\alpha_a & 0 \\ \cos 2\alpha_a & \cos^2 2\alpha_a & \cos 2\alpha_a \sin 2\alpha_a & 0 \\ \sin 2\alpha_a & \cos 2\alpha_a \sin 2\alpha_a & \sin^2 2\alpha_a & 0 \\ 0 & 0 & 0 & 0 \end{bmatrix} \tag{3}$$

$$S_{in} = \begin{bmatrix} 1 \\ \cos 2\alpha_p \\ \sin 2\alpha_p \\ 0 \end{bmatrix}, \tag{4}$$

where α_a is the transmission angle of the analyzer, and θ is the Faraday rotation.

Considering linearly horizontally polarized ($\alpha_p = 0$) monochromatic input beam and combining the Eqs. (1)–(4), the expression for detected intensity of the out put beam is given by

$$I = \frac{I_0}{2}\left[1 + \cos 2(\theta - \alpha_a)\right] \tag{5}$$

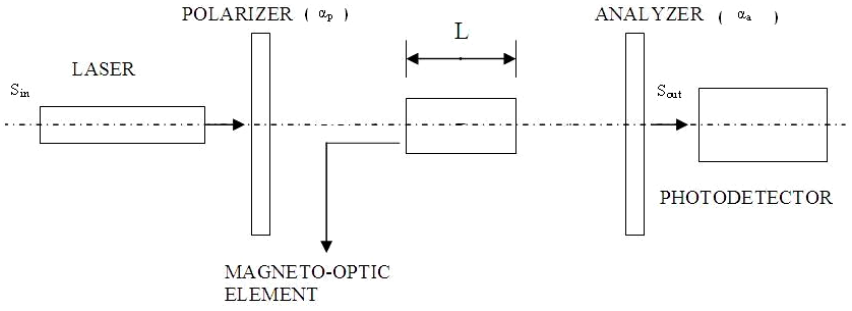

Fig. 1. Basic schematic diagram of the magneto-optic measurement set up.

when a linearly polarized light passes through a magneto optic medium in a direction parallel to the uniform magnetic field, the Faraday rotation is given by the relation [36]

$$\theta = V_{ver\,\det} LB, \tag{6}$$

where, V_{Verdet}, L and B are the wavelength dependent Verdet constant of the TDG element, length of the magneto-optic medium and magnetic flux density of the permanent magnet respectively. In order to improve the response and avoid the effect of intensity variation of incident light, the measurement setup utilizes the dual quadrature polarimetric detection scheme in reflection mode where the intensity of the output beam is measured for α_a = +45° and -45° and the ratio of the difference over sum is evaluated [25].

Thus substituting α_a = +45° and -45° in Eq. (5) and taking the ratio of difference over sum, the expression for power ratio (PR) is obtained as

$$PR = \frac{I_{+45} - I_{-45}}{I_{+45} + I_{-45}} = \sin(2\theta) \tag{7}$$

In a double pass mode the expression for power ratio will be

$$PR = \sin(4\theta) \tag{8}$$

3. Experiment and Discussions

The dual quadrature polarimetric scheme [25] is shown in Fig. 2.

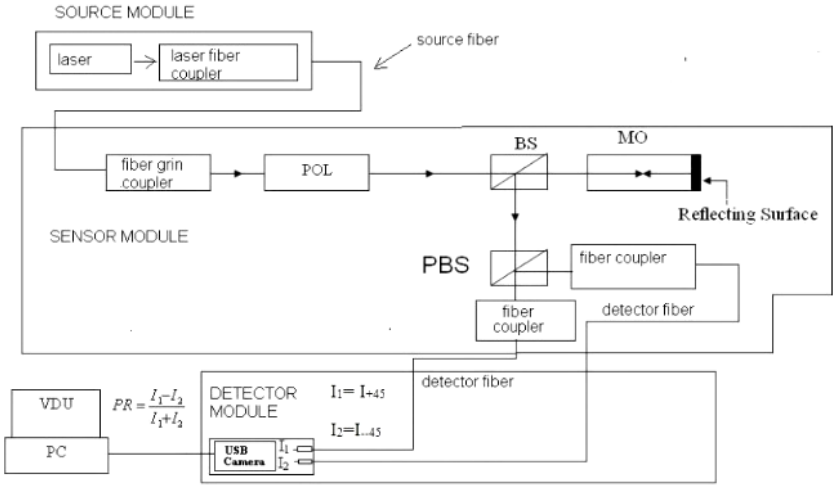

Fig. 2. The dual quadrature polarimetric scheme of the magneto-optic sensor.

In source module the light from a 5 mW DPSS (diode pumped solid state) laser (wavelength 0.5435 μm) is coupled to a multimode optical fiber (source fiber) by a laser fiber coupler with the help of microscope objective. The other end of the fiber is coupled to the fiber GRIN lens coupler of the sensor module for producing collimated laser beam. The beam passes through a polarizer (POL) and then through a beam splitter (BS) to the magneto-optic (MO) TDG rod of length 30 mm and diameter 10 mm. The reflected beam from the mirrored surface of the magneto-optic (MO) element then passes through the polarizing beam splitter (PBS). The two light beams with orthogonal polarization are then coupled to two multimode optical fibers (detector fibers) with the help of two microscope objective based fiber laser couplers. The other ends of the detector fibers mounted in fiber chucks are focused on to the CCD sensor surface in an USB based camera detector. The advancement in digital image processing, availability of high speed computer with high memory size, simple image grabbing techniques and simplified image storage, manipulation and display enables the use of CCD camera as a light detector in place of single photo detector [37-39] The light intensities I_1 and I_2 are obtained as average gray values of the spot images produced by the camera detector and the power ratio (PR) is measured with the help of the relation PR = $(I_1 - I_2)/ (I_1 + I_2)$. Figs. 3-5 shows the photographs of prototype source, sensor and camera detector units mounted on non-magnetic base plates (PMMA materials). For online measurement of PR, application software is developed in LabView utilizing IMAQ vision tools. The sensor system is first tested in the laboratory by inserting the TDG cylinder inside the core of a multiple layer solenoid coil (copper) of length 95 mm and with 2600 turns.

Fig. 6 (a) shows the variation of PR with the variation of current (DC) through the solenoid coil. The variation of magnetic flux density with the variation of coil current is also measure by the axial Hall probe of a calibrated Gauss meter and a maximum linear change of around 35 mT is obtained when the current is changed from 0 to 2 Amp. Fig. 6 (b) shows the image of the fiber tips acquired

in LabView for calculating the light intensities I_1 and I_2 from the average gray values within the respective region of interest.

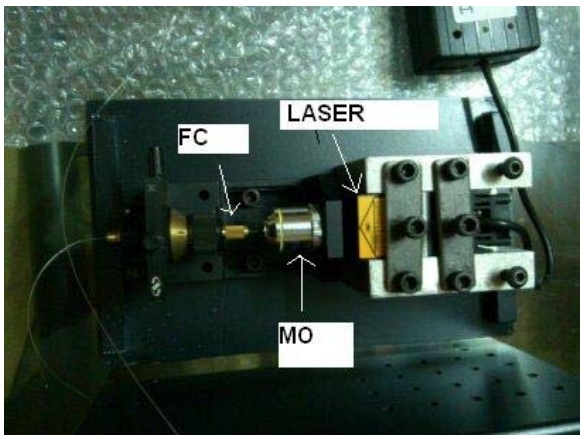

Fig. 3. Source module mounted on the base plate.

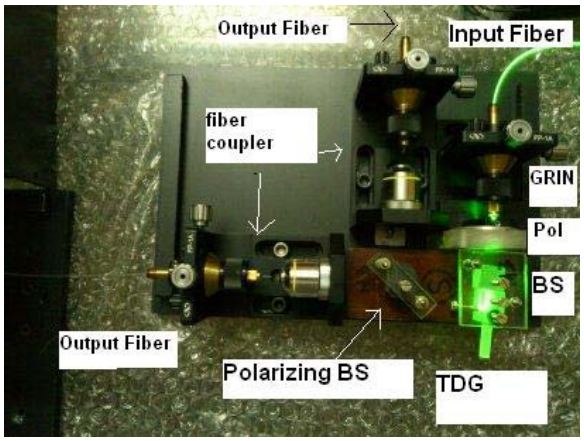

Fig. 4. Sensor module mounted on the base plate.

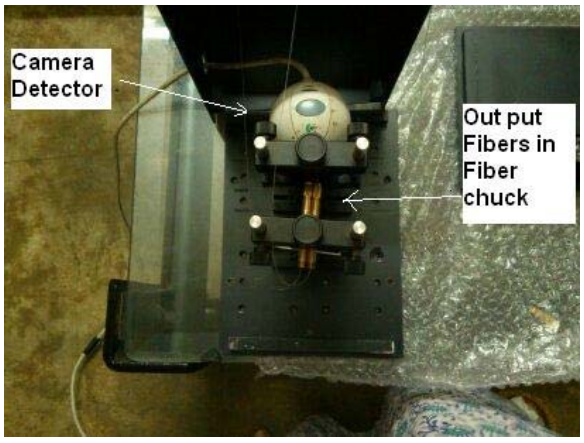

Fig. 5. Detector module mounted on the base plate.

Fig. 7 shows the experimental setup for sensing the DC motor field winding. The magneto-optic TDG element is located at a distance 10 mm from DC motor field winding and input current to the field winding is increased slowly from 1 ampere to 7 ampere in steps of 0.5 Ampere. The experiment is repeated for increasing and decreasing current. For comparison with the data obtained from magneto-optic setup an axial Hall probe of a calibrated gauss meter is also used to sense the magnetic flux density variation as the current changes. The resulting PR is obtained by using Eq. 6 and 8 and considering TDG element of length L=30 mm and verdet constant V_{verdet} = 101.81 rad/T.m at λ=0.5435 μm [31]. In the measurement process the residual magnetism of 0.01K gauss in the field winding is obtained.

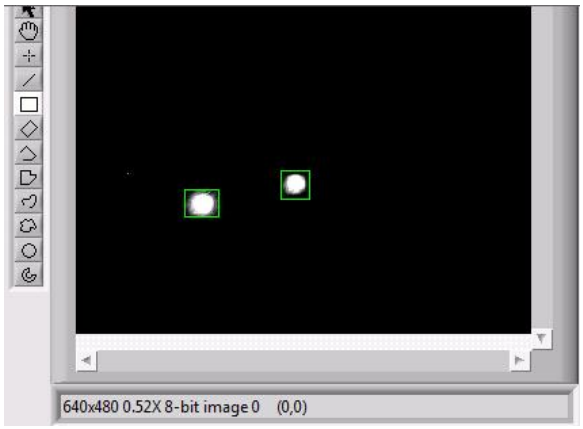

(a)

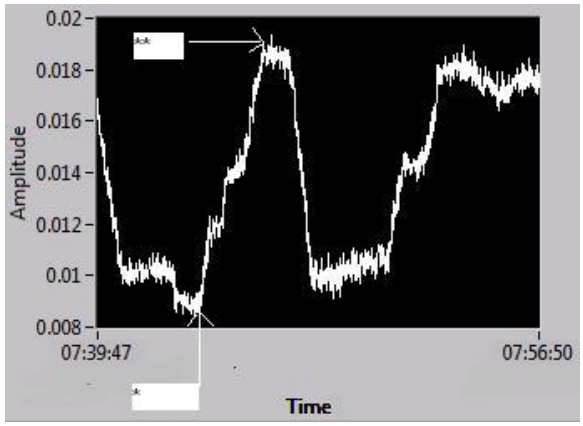

(b)

Fig. 6. Testing with a solenoid current of 2 Amps in laboratory. (a) Shows the variation of PR with time when the solenoid coil current is changed from 0 -2 Amp. At point * the coil current is practically zero and at point ** the coil current is 2 Amps (b) Shows the image of the detector fiber tips surrounded by region of interest for calculating the average gray value.

Curve A of Fig. 8 shows the average of ten measurements using magneto-optic sensor element and for both ascending and descending order of current. Curve-C shows the linear fit of Curve-A with sum of the square of errors (SSE) =9.662e-005 and

R-square=0.9778. Curve-B of Fig. 8 shows the average of five measurements using Hall sensor probe and for both ascending and descending order of current. Curve-D shows the linear fit of Curve-B with sum of the square of errors (SSE)= 5.325e-006 and R-square=0.9929.

Fig. 7. Experimental setup for detecting the change in coil current in the field winding of a DC motor.

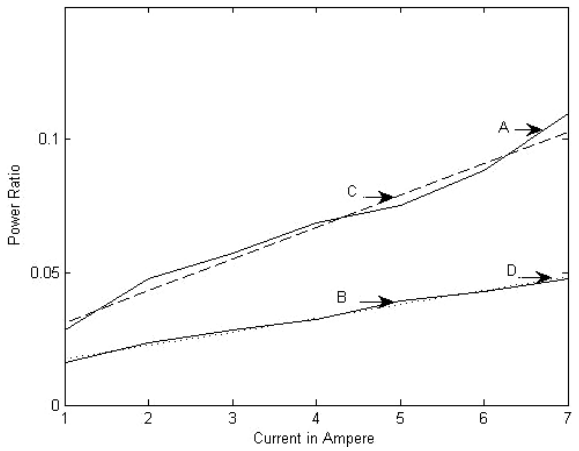

Fig. 8. Variation of Power Ratio (PR) with the variation of coil current (of field windings). Curve-A (─) shows the variation obtained with magneto-optic TDG element and Curve-C (─ ─) shows the linear fit of Curve-A. Curve-B (─) shows the variation obtained with a Hall magnetic sensor and Curve-D (….) shows the linear fit of Curve-B.

Both the curves show a fairly linear variation over a wide range of current passing through the field winding. Interestingly we note that the sensitivity of the magneto-optic sensor is practically more than double the sensitivity of Hall probe sensor since the slopes of the Curves C and D are 40° and 17° respectively. The difference between Curve-A and B can be explained by the improper polarizer setting ("Pol" in Fig. 4) of input polarizer with transmission angle α_p which we have considered as linearly horizontally polarized i.e. $\alpha_p = 0°$. With the finite value of α_p the expression for Power Ratio (PR) will be changed to PR= sin $(4\theta+2\alpha_p)$. The magneto-optic sensor developed can further be miniaturized by replacing the bulky fiber coupler (Fig. 4) with a lens and molded plastic packaging.

Acknowledgements

This work was supported by Department of Science and Technology (DST), Govt. of India, New Delhi. Authors are grateful to BIT management for support and encouragement.

References

[1]. K. S. Lion, Instrumentation in Scientific Research: Electrical Input Transducers, *McGraw-Hill*, New York, 1959.
[2]. H. R. Everett, Sensors for Mobile Robots: Theory and Application, *A K Peters, Ltd.,* Wellesley, Massachusetts, 1995.
[3]. J. E. Lenz, A review of magnetic sensors, in *Proceedings of the IEEE,* Vol. 78, Issue 6, 1990, pp. 973–989.
[4]. LEMI web portal (http://www.lemisensors.com).
[5]. Lakeshore web portal (http://www.lakeshore.com).
[6]. MEDA web portal (http://www.meda.com).
[7]. W. Bartsch, G. Rupp, W. Schelter, Photolithographic structuring of giant magnetoresistive Co-Cu multilayers, *Sensors and Actuators A: Physical*, Vol. 46, Issue 1-3, 1995, pp. 302-306.
[8]. Honeywell web portal (http://www51.honeywell.com/aero/common/documents/myaerospacecatalog-documents/Missiles-Munitions/Sensors_Product__Catalog.pdf).
[9]. Y. Chong, Y. U. Jun, Z. Wen-Li, W. Yun-Bo, X. Ji-Fan, G. Jun-Xiong, Giant magnetic resistor sensor, *Electronic Components & Materials,* Vol. 19, Issue 5, 2000, pp. 32-34.
[10]. Instrument Engineer's Handbook, Process Measurement and Analysis, 4th Edition, Vol. 1, B. G. Liptak (Ed.), *CRC Press*, New York, 2003.
[11]. J. P. Bentley, Principles of Measurement Systems, 3rd Edition, *Longman,* Singapore, 1995.
[12]. E. O. Doeblin, Measurement System Application and Design, 4th Edition, *McGraw-Hill*, New York, 1990.
[13]. Handbook of Optics, Vol. II, 2nd Edition, Michael Bass (Editor-in-Chief), *McGraw-Hill*, New York, 1995.
[14]. D. M. Considine, Process Instruments and Control Hand Book, 2nd Edition, *McGraw-Hill*, New York, 1974.
[15]. MICRO-EPSILON web portal (http://www.micro-epsilon.com).
[16]. F. A. Jenkins, H. E. White, Fundamentals of Optics, 4th Edition, *McGraw-Hill*, New York, 1976.
[17]. H. Sohlstrom, Fiber optic magnetic field sensors utilizing iron garnet materials, Ph. D. Thesis, *Royal Institute of Technology (KTH),* Stockholm, 1993.
[18]. Y. H. Jeon, J. W. Lee, J. H. Oh, J. C. Lee, S. C. Choi, Magneto-optical properties of Bi-YIG

nanoparticles/epoxy hybrid materials, *Physica Status Solidi (A) Applied Research*, Vol. 201, Issue 8, 2004, pp. 1893–1896.
[19]. LEOS web portal (http://photonicssociety.org/newsletters/apr03/university.html).
[20]. B. Yi, B. C. B. Chu and K. S. Chiang, Magneto-optical electric current sensor with enhanced sensitivity, *Measurement Science and Technology*, Vol. 13, Issue 7, 2002, pp. N61-N63.
[21]. R. H. Stolen and E. H. Turner, Faraday rotation in highly birefringent optical fibers, *Applied Optics*, Vol. 19, Issue 6, 1980, pp. 842-845.
[22]. P. R. Forman and F. C. Jahoda, Linear birefringence effects on fiber-optic current sensors, *Applied Optics*, Vol. 27, Issue. 15, 1988, pp. 3088-3096.
[23]. T. Yoshino, K. Minegishi and M. Nitta, A very sensitive Faraday effect current sensor using a YAG/ringcore transformer in a transverse configuration, *Measurement Science and Technology*, Vol. 12, Issue 7, 2001, pp. 850-853.
[24]. D. Alasia, L. Thevenaz, A novel all-fiber configuration for a flexible polarimetric current sensor, *Measurement Science and Technology*, Vol. 15, Issue 8, 2004, pp. 1525-1530.
[25]. Optical Fiber Sensor Technology, Vol. 3, Chapter 7, Edited by K. T. V. Grattan, B. T. Meggit, *Kluwer Academic Publishe*rs, 1998, London,.
[26]. G. B. Gillman, A reliable faraday rotator with solid state switching, *Journal of Physics E: Scientific Instruments*, Vol. 10, Issue 10, 1977, pp. 959–960.
[27]. R. Yasuhara, S. Tokita, J. Kawanaka, T. Kawashima, H. Kan, H. Yagi, H. Nozawa, T. Yanagitani, Y. Fujimoto, Y. Yoshida, M. Nakatsuka, Development of cryogenic TGG ceramic based Faraday rotator for inertial fusion driver, *Journal of Physics.: Conference Series*, Vol. 112, Issue 3, 2008.
[28]. J. D. Mansell, J. Hennawi, E. K. Gustafson, M. M. Fejer, R. L. Byer, D. Clubley, S. Yoshida, D. H. Reitze, Evaluating the effect of transmissive optic thermal lensing on laser beam quality with a Shack-Hartmann wave-front sensor, *Applied Optics*, Vol. 40, Issue 3, 2001, pp. 366–374.
[29]. W. Li, K. Zou, M. Lu, B. Peng, W. Jhao, Faraday glasses with a large size and high performance, *International Journal of Applied Ceramic Technology*, Vol. 7, Issue 3, 2010, pp. 369–374.
[30]. D. Goldring, Z. Zalevsky, G. Shavtay, D. Abharam, D. Mendlovic, Magneto-optic based devices for polarization control, *Journal of Optics A: Pure Applied Optics*, Vol. 6, Issue 1, 2004, pp. 98–105.
[31]. S. Chakraborty, S. C. Bera, Magneto-optic over-current detection with null optical tuning, *Sensors & Transducers*, Vol. 87, Issue 1, January 2008, pp. 52–62.
[32]. S. Chakraborty, S. C. Bera, Color signature of current: a novel concept for current level indication, *Sensors & Transducers,* Vol. 93, Issue 6, June 2008, pp. 57–68.
[33]. S. Chakraborty, S. C. Bera, Design of stokes polarimeter using rotators, *Journal of Optics*, Vol. 39, Issue 2, 2010, pp. 82–89.
[34]. S. Chakraborty, S. C. Bera, A. K. Chakraborty, Simulation of a polarization pupil filter with magneto-optic lens under elliptically polarized illumination, *Optik – International Journal for Light and Electron. Optics*, Vol. 122, Issue 6, 2011, pp. 549–552.
[35]. S. C. Bera, S. Chakraborty, Study of Magneto-Optic Element as a Displacement Sensor, *Measurement*, Vol. 44, Issue 9, 2011, pp. 1747-1752.
[36]. K. Lizuka, Engineering Optics, 2nd Edition, *Springer-Verlag*, Berlin, 1983.
[37]. E. Sanchez-Ortiga, C. J. R. Sheppard, G. Saavedra, M. Martínez-Corral, A. Doblas, and A. Calatayud, Subtractive imaging in confocal scanning microscopy using a CCD camera as a detector, *Optics Letters*, Vol. 37, Issue 7, 2012, pp. 1280-1282.
[38]. Nikon web portal (www.microscopyu.com/print/articles/digitalimaging/digitalintro-print.html).
[39]. B. Chakraborty, Effect of camera gamma and gain on the line shape and axial resolution in a confocal microscope setup, *Journal of Optics*, Vol. 34, Issue 1, 2014, pp. 42-47.